THE JOURNAL OF BIOLOGICAL CHEMISTRY
Vol. 279, No. 14, Issue of April 2, pp. 14111–14119, 2004
Printed in U.S.A.

Aggregation of the Acylphosphatase from *Sulfolobus solfataricus*

THE FOLDED AND PARTIALLY UNFOLDED STATES CAN BOTH BE PRECURSORS FOR AMYLOID FORMATION*

Received for publication, November 28, 2003, and in revised form, December 23, 2003
Published, JBC Papers in Press, January 14, 2004, DOI 10.1074/jbc.M312961200

Georgia Plakoutsi, Niccolò Taddei, Massimo Stefani, and Fabrizio Chiti‡

From the Dipartimento di Scienze Biochimiche, Università di Firenze, Viale Morgagni 50, 50134 Firenze, Italy

Protein aggregation is associated with a number of human pathologies including Alzheimer's and Creutzfeldt-Jakob diseases and the systemic amyloidoses. In this study, we used the acylphosphatase from the hyperthermophilic Archaea *Sulfolobus solfataricus* (Sso AcP) to investigate the mechanism of aggregation under conditions in which the protein maintains a folded structure. In the presence of 15–25% (v/v) trifluoroethanol, Sso AcP was found to form aggregates able to bind specific dyes such as thioflavine T, Congo red, and 1-anilino-8-naphthalenesulfonic acid. The presence of aggregates was confirmed by circular dichroism and dynamic light scattering. Electron microscopy revealed the presence of small aggregates generally referred to as amyloid protofibrils. The monomeric form adopted by Sso AcP prior to aggregation under these conditions retained enzymatic activity; in addition, folding was remarkably faster than unfolding. These observations indicate that Sso AcP adopts a folded, although possibly distorted, conformation prior to aggregation. Most important, aggregation appeared to be 100-fold faster than unfolding under these conditions. Although aggregation of Sso AcP was faster at higher trifluoroethanol concentrations, in which the protein adopted a partially unfolded conformation, these findings suggest that the early events of amyloid fibril formation may involve an aggregation process consisting of the assembly of protein molecules in their folded state. This conclusion has a biological relevance as globular proteins normally spend most of their lifetime in folded structures.

Protein aggregation is a hallmark of a number of human pathologies including Alzheimer's, Parkinson's, and Creutzfeldt-Jakob diseases and the systemic amyloidoses associated with immunoglobulin light chain, transthyretin, lysozyme, and β_2-microglobulin (1). Under these pathological conditions, a protein or peptide that is normally soluble deposits into fibrillar aggregates commonly referred to as amyloid fibrils; these display a diameter of 7–13 nm, an extensive β-sheet structure, and characteristic staining properties such as a Congo red birefringence under cross-polarized light (2).

It has long been recognized that the conformational state of a polypeptide chain that forms the precursor aggregates, eventually leading to amyloid formation, is neither the natively folded nor the fully unfolded state but a partially folded state that contains significant structure, although lacking a well defined tertiary fold (3, 4). For the majority of the proteins that have been studied in detail, it is clear that this is the case. Fibril formation from transthyretin, for example, occurs preferentially at mildly acidic pH values (5). Under these conditions the native tetrameric conformation of the protein is found to dissociate and to partially unfold, thus adopting a conformation that is highly prone to aggregate and to form amyloid fibrils (5). Similarly, β_2-microglobulin forms amyloid fibrils under conditions in which the N- and C-terminal β-strands of the protein are unfolded (6). Observations that these regions of the sequence are solvent-exposed in the fibrils formed from this protein provide direct evidence that fibril formation does not originate from the assembly of protein molecules in their native conformation (7). Some other proteins such as cystatin C, which is associated with a hereditary form of cerebral amyloid angiopathy, and the cell cycle regulatory protein p13suc1 are suggested to fibrillize via domain swapping (8, 9). Domain swapping is a mechanism in which part of the structure of each monomer replaces the corresponding structural elements of an identical monomer so as to form an oligomer where each subunit has a similar structure to the folded monomer (8, 9). Even in this case, aggregation is proposed to require a substantial unfolding of the folded monomer in order to facilitate exchange of structural elements (8, 9). The presence of structure in the fibrils formed from the amyloid β peptide associated with Alzheimer's disease indicates that fibrils formed from peptides or proteins that are unstructured in their soluble form need to adopt a partially structured conformation either before or during assembly (10, 11).

These are just a few examples that support the "conformational change hypothesis" of fibril formation. Nevertheless, the general validity of these theories has been challenged by a number of recent findings. On the one hand, amyloid formation may occur readily from peptides as short as 5 residues, where formation of structure before assembly is rather unlikely given the short length of the peptides (12). On the other hand, a number of observations have indicated that fibrillar aggregates may originate from the assembly of globular protein molecules in their native or native-like state (13, 14). The yeast prion Ure2p was shown to form fibrils that display birefringence upon Congo red binding and increased resistance to proteinase K treatment, typical of amyloid fibrils (15–17). It was shown that Ure2p retains its native α-helical content and ability to

* This work was supported by a fellowship from the European Union (to G. P.), by grants from the European Union (Project "Protein Folding, Misfolding, Aggregation, and Disease"), the Italian MIUR (FIRB Project "Protein Folding: the Second Half of the Genetic code"; PRIN Project "Folding e Misfolding di Proteine: Biogenesi, Struttura e Citotossicità di Aggregati Proteici"), the Italian CNR (L. 449/97, Sector "Genomica Funzionale; Project "Strutture ed Interazioni Molecolari di Prodotti Genici"), and the Cassa di Risparmio di Firenze (Project: Studio dei Meccanismi Molecolari alla Base dell'Aggregazione Proteica e della Formazione delle Fibrille Amiloidi). The costs of publication of this article were defrayed in part by the payment of page charges. This article must therefore be hereby marked "*advertisement*" in accordance with 18 U.S.C. Section 1734 solely to indicate this fact.

‡ To whom correspondence should be addressed. Tel.: 39-055-413765; Fax: 39-055-4222725; E-mail: fchiti@scibio.unifi.it.

bind glutathione after assembly into fibrils (13). Accordingly, x-ray fiber diffraction analysis has shown that the fibrils do not possess a cross-β-structure (18). Similarly, lithostathine, a protein that forms both independent and colocalized deposits with amyloid β plaques, neurofibrillary tangles, and PrP^{sc} plaques, maintains its native content of secondary structure, although it aggregates into fibrillar structures (14). In this case the resulting proteinase K-resistant fibrils do not bind Congo red in addition to showing no cross-β-structure (14). The ability of these two proteins to form fibrillar structures under non-denaturing conditions close to a physiological medium suggests that a substantial unfolding is not required (13, 14).

Amyloid formation is a property that is not only shared by a few polypeptide chains associated with disease. Following the initial observation that the Src homology 3 domain from phosphatidylinositol 3-kinase is able to form fibrillar aggregates structurally indistinguishable from those formed naturally under pathological conditions (19), ~20 proteins were shown to have the potential to form amyloid fibrils under appropriate conditions *in vitro* (1). In addition to a rise in general awareness that protein sequences, and more generally the biology of cells, have evolved structural adaptations and biological mechanisms to effectively defend from undesired protein aggregation, these findings have provided new model systems to investigate the fundamentals of protein aggregation (1). Amyloid formation from these non-pathological systems occurs under mild denaturing conditions, such as at low pH values, at high temperatures and in the presence of organic cosolvents. Moreover, mutations that destabilize the native conformation of a protein increase its propensity to aggregate (20, 21). These observations support further the view that substantial unfolding of the compact globular state of a protein is generally the first conformational change that initiates aggregation.

In this study, we show that aggregation of one of these non-pathological proteins may result from a conformational state that presents only minor structural modifications compared with the native form of the protein. The protein that we have used is the acylphosphatase from the hyperthermophile Archaea *Sulfolobus solfataricus* (Sso AcP).[1] A stable protein from a hyperthermophilic organism is likely to maintain its native topology under a wide range of conditions, including relatively harsh solvent conditions that normally promote aggregation. Utilization of a hyperthermophilic protein therefore allows aggregation processes to be investigated under conditions in which the native conformation is not significantly disrupted. Although the native structure of Sso AcP has not yet been resolved, the relatively high sequence identity with the previously characterized human muscle and common-type acylphosphatases and the N-terminal domain of the *Escherichia coli* HypF suggests it may display the same basic ferredoxin-like topology, consisting of a five-stranded antiparallel β-sheet facing two antiparallel α-helices (22–24). In addition to illustrating the capability of this protein to form ordered aggregates, we will present kinetic evidence that aggregation originates from a conformational state that retains enzymatic activity and is located on the native side of the major free energy barrier of unfolding.

EXPERIMENTAL PROCEDURES

Materials—Thioflavine T (ThT), Congo red, 1-anilino-8-naphthalenesulfonic acid (ANS), guanidine hydrochloride (GdnHCl), and 2,2,2-trifluoroethanol (TFE) were purchased from Sigma. Benzoyl phosphate was synthesized and purified as described (25).

Cloning, Expression, and Purification of Sso AcP—The DNA fragment corresponding to the Sso AcP gene, originally inserted in a pEMBL plasmid, was amplified by PCR using two primers that contained the restriction sites for BamHI and EcoRI. The resulting amplified fragments were purified using the QiaQuick Purification Kit by Qiagen (Milano, Italy), digested with BamHI and EcoRI for 2 h, purified again, and then ligated into pGEX-2T plasmid, previously digested with the same restriction enzymes. The resulting plasmid was checked by DNA sequencing and then transformed into *E. coli* DH5α cells. Gene expression in the DH5α cells and purification of the resulting protein were carried out as described for human muscle acylphosphatase (26). Protein purity was checked by SDS-PAGE and electrospray mass spectrometry. The resulting protein sequence is GSMKKWSDTEVFEMLKRMYARVYGLVQGVGFRKFVQIHAIRLGIKGYAKNLPDGSVEVVAEGYEEALSKLLERIKQGPPAAEVEKVDYSFSEYKGEFEDFETY. The Gly-Ser dipeptide at the N terminus results from the cloning in pGEX-2T. The underlined Met residue is residue 1. Purified protein was stored in 10 mM Tris, pH 8.0. Protein concentration was determined by UV absorption using an ϵ_{280} value of 1.26 ml mg^{-1} cm^{-1}.

Thioflavine T Assay—Sso AcP was incubated at a concentration of 0.4 mg ml^{-1} for 2 h in 50 mM acetate buffer, pH 5.5, 25 °C in the presence of various concentrations of TFE. 60 μl of each sample were added to 440 μl of a solution containing 25 μM ThT, 25 mM phosphate buffer, pH 6.0. The fluorescence of the resulting samples was measured at 25 °C using a 2 × 10-mm path length cuvette and a PerkinElmer LS 55 spectrofluorimeter equipped with a thermostated cell compartment. The excitation and emission wavelengths were 440 and 485 nm, respectively. The kinetics of aggregation of Sso AcP were studied by incubating the protein under the same conditions of pH and temperature in 15, 20, 25, 50, and 70% of TFE (v/v). Aliquots were withdrawn at regular time intervals and used for the ThT assay as described above. In order to determine the rate constants of aggregation (k), the plots of the fluorescence intensity *versus* time were fit to single exponential functions of the form $y = q + A \exp(-kt)$.

Congo Red Assay—Sso AcP was incubated at a concentration of 0.4 mg ml^{-1} for 30 min in 50 mM acetate buffer, pH 5.5, 25 °C in the presence of 0, 20, 50, or 70% (v/v) TFE. Aliquots of 60 μl of each protein solution were mixed with 440 μl of solutions containing 20 μM Congo red, 5 mM phosphate buffer, 150 mM NaCl, pH 7.4. After a 2–3-min equilibration, optical absorption spectra were acquired from 400 to 700 nm by an Ultrospec 2000 UV-visible spectrophotometer (Amersham Biosciences). A 4 × 5-mm path length cuvette was used. Solutions without protein and solutions without Congo red were used as controls.

ANS Assay—Sso AcP was incubated for 30 min at 25 °C as described above for the ThT assay. Aliquots of 60 μl of the protein solutions were mixed with 440 μl of solutions containing 1 mM ANS, in 50 mM acetate buffer, pH 5.5, 25 °C. Fluorescence spectra were acquired using the PerkinElmer LS 55 spectrofluorimeter, an excitation wavelength of 390 nm, and an emission range from 410 to 620 nm. A 2 × 10-mm path length cell was used.

Dynamic Light Scattering—Sso AcP was incubated for 30 min as described above for the ThT assay. Size distributions of the protein samples by intensity were obtained before and after centrifugation of the samples (18,000 rpm for 10 min). The data were attained using a Zetasizer Nano S dynamic light scattering (DLS) device from Malvern Instruments (Malvern, Worcestershire, UK). The temperature was maintained at 25 °C by a thermostating system. Low volume 12.5 × 45-mm disposable cells were used. The buffer was filtered immediately before use to eliminate any impurities.

Far-UV Circular Dichroism—Sso AcP was incubated for 30 min as described above for the ThT assay. Far-UV CD spectra were acquired at 25 °C using a cuvette of 1-mm path length and a Jasco J-810 spectropolarimeter (Great Dunmow, Essex, UK) equipped with a thermostated cell holder. Each spectrum was recorded as the average of three scans. The first set of spectra for the samples was acquired after an incubation of 30 min at 25 °C. A second set of spectra was acquired after centrifugation of the samples at 18,000 rpm for 10 min. In the kinetic experiment the far-UV ellipticity at 222 nm was monitored for Sso AcP at 0.4 mg ml^{-1} in 20% (v/v) TFE at 25 °C for 1 h.

Electron Microscopy—Electron micrographs were acquired by a Joel JEM 1010 transmission electron microscope (Tokyo, Japan) at 80-kV excitation voltage. The samples consisted of 0.4 mg ml^{-1} Sso AcP incubated for 1 h at 25 °C in 50 mM acetate buffer, pH 5.5, in the absence or presence of 20% (v/v) TFE. 3 μl of the sample were placed on a Formvar and carbon-coated grid from Agar Scientific (Stansted, Essex, UK) for 3–5 min and then blotted off. 3 μl of 2% uranyl acetate were then added, remained on the grid for 3 min, and blotted off. The magnification was 20,000–30,000 times.

[1] The abbreviations used are: Sso AcP, *S. solfataricus* acylphosphatase; ANS, 1-anilino-8-naphthalenesulfonic acid; DLS, dynamic light scattering; GdnHCl, guanidine hydrochloride; TFE, 2,2,2-trifluoroethanol; ThT, thioflavine T.

Enzymatic Activity Measurements—Sso AcP was incubated at a concentration of 0.03 mg ml^{-1} for 30 min in 50 mM acetate buffer, pH 5.5, 25 °C. Incubation was carried out as follows: (i) in the presence of various concentrations of TFE, (ii) in the absence of TFE, and (iii) in the presence of 6 M GdnHCl. After pre-incubation, enzymatic activity was measured spectrophotometrically using benzoyl phosphate as a substrate (25). Briefly, 50 μl of the protein sample were mixed with 950 μl of a solution containing 2.5 mM benzoyl phosphate, 50 mM acetate buffer, pH 5.5, and various TFE concentrations. Final protein concentration was 0.0015 mg ml^{-1}. For the first set of experiments (i) the protein sample was pre-incubated in the same TFE concentration that was used afterward for the enzymatic activity assay. All recorded enzymatic activity values were subtracted by the spontaneous, non-catalyzed hydrolysis of benzoyl phosphate measured under the same conditions.

Stopped-flow Kinetics—Folding and unfolding of Sso AcP were followed with a Bio-logic SFM-3 stopped-flow device coupled to a fluorescence detection system (Claix, France) and thermostated with a water-circulating bath. The excitation wavelength was 280 nm, and the emitted fluorescence above 320 nm was monitored using a bandpass filter. For the unfolding experiments, 1 volume of 0.4 mg ml^{-1} Sso AcP in buffer was mixed with 19 volumes of a solution containing TFE. Folding was initiated by mixing 1 volume of 0.4 mg ml^{-1} Sso AcP denatured in 6 M GdnHCl with 19 volumes of a solution without GdnHCl and containing low concentrations of TFE. The final conditions were 0.02 mg ml^{-1} Sso AcP, 50 mM acetate buffer, pH 5.5, 25 °C, and the final TFE concentration range was from 45 to 60% (v/v) (for unfolding) or from 0 to 18% (v/v) (for folding). The dead time was generally 10.4 ms. The kinetic traces were fitted to simple exponential functions of the form shown in Equation 1,

$$y(t) = at + b + A\exp(-kt) \quad \text{(Eq. 1)}$$

where $y(t)$ is the fluorescence signal recorded as a function of time; A and k are the amplitude and rate constant, respectively. The additional straight line $a\ t + b$ was considered to account for trends of the fluorescence signal arising due to aggregation, proline isomerization, fluorescence decay of the sample, and other disturbing factors.

RESULTS

Aggregation of Sso AcP was promoted by adding TFE. In addition to be a cosolvent commonly used to promote amyloid formation (20, 27, 28), TFE has also proven useful for revealing details of the mechanism of protein aggregation (29–31). For the study of aggregation of Sso AcP, we focused on the first aggregational events, *i.e.* the conversion of the soluble form into pre-fibrillar aggregates. Indeed, several studies suggest that these pre-fibrillar structures may be the key oligomeric species that are toxic to the cells and responsible for the onset of neurodegenerative diseases (27, 32–34).

Aggregate Formation Monitored by Dye Binding—Sso AcP was incubated for 2 h at 25 °C, pH 5.5, in various TFE concentrations. The samples were then subjected to the ThT assay so as to reveal the presence of aggregates with a relatively ordered organization (35). Although the samples incubated in the absence or presence of low TFE concentrations did not show an increase in ThT fluorescence, samples incubated at TFE concentrations in the range of 15–35% (v/v) produced a 6-fold increase (Fig. 1). TFE concentrations higher than 40% (v/v) led to a decrease in fluorescence intensity, yet not reaching values of zero. At the highest TFE concentration used (70% (v/v)), the intensity was about half of the maximum value.

ANS is a hydrophobic dye that binds to solvent-exposed hydrophobic surfaces of a polypeptide chain (36). Whereas folded or unfolded states of proteins exhibit very weak binding affinity, conformational states with clusters of exposed hydrophobic groups feature a much higher affinity allowing this dye to serve as a marker for partially folded states (36). Recent reports (37) have shown that aggregates of the amyloid β peptide able to interact with the lipid bilayer of cell membranes are also able to bind and increase the fluorescence of ANS, most probably as a result of the exposure of hydrophobic clusters on the surface of these aggregated structures.

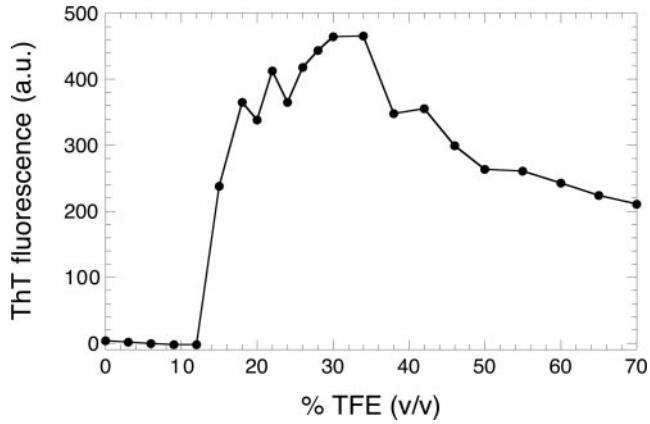

FIG. 1. **Fluorescence intensity of ThT at 485 nm upon binding to Sso AcP pre-incubated in various concentrations of TFE.** The protein samples were incubated for 2 h at 25 °C, pH 5.5, at the indicated TFE concentrations. The values reported in the figure for each concentration of TFE were obtained by subtracting the ThT fluorescence measured in the absence of protein at the corresponding TFE concentrations. *a.u.*, arbitrary units.

Sso AcP was incubated for 30 min under the same conditions used for the ThT measurements. The samples were then used for the ANS assay. At TFE concentrations in the 15–25% (v/v) range, the ANS fluorescence emission was remarkably more intense than that of samples containing no protein (Fig. 2). Furthermore, under these conditions the ANS emission spectra appeared to have a maximum shifted from the wavelength of 515 nm, observed for free ANS, to that of 480 nm (Fig. 2*A*). Removal of the aggregates from the sample by centrifugation reduced almost completely the ability of the sample to increase the fluorescence of ANS. Therefore, the observed increase of ANS fluorescence is attributable to the binding of this dye to the aggregates, rather than to partially folded states that could possibly be present in the sample.

Congo red spectra were also monitored in the presence of Sso AcP. The protein was pre-incubated for 30 min under the same conditions of temperature and pH and in the presence of 0, 20, 50, and 70% (v/v) TFE. Upon the binding of Congo red to ordered aggregates, the absorption maximum of the dye undergoes a red shift from 490 to ~540 nm (38). The spectra of Congo red obtained in the absence or in the presence of Sso AcP pre-incubated in buffer were highly superimposable, both presenting a maximum at 490 nm (Fig. 3*A*). By contrast, the spectrum obtained in the presence of Sso AcP, pre-incubated in 20% TFE, had an optical absorption higher than the control spectrum recorded in the absence of protein, throughout the whole wavelength range (Fig. 3*B*). This originated from the considerable light scattering produced by the protein that yielded an apparently increasing optical absorption as the wavelength decreased (Fig. 3*B*). The difference spectrum at 20% TFE, obtained by subtracting the spectra of the protein alone and of Congo red alone from the spectrum of the protein in the presence of Congo red, exhibited a maximum at ~550 nm (Fig. 3*C*). No apparent maxima were obtained in the difference spectra at the remaining concentrations of TFE (Fig. 3*C*).

Overall, the analysis carried out with ThT, Congo red, and ANS indicate the presence of ordered aggregates within the range 15–25% (v/v) TFE. Less ordered aggregated species seem to be present at higher TFE concentrations, whereas no aggregation seems to occur significantly at concentrations of TFE lower than 15% (v/v), at least on the time scale investigated here.

Aggregate Formation Monitored by Dynamic Light Scattering—The evaluation of the presence and size of Sso AcP aggregates was achieved by a DLS analysis. The protein was incubated in various TFE concentrations ranging from 0 to 70%

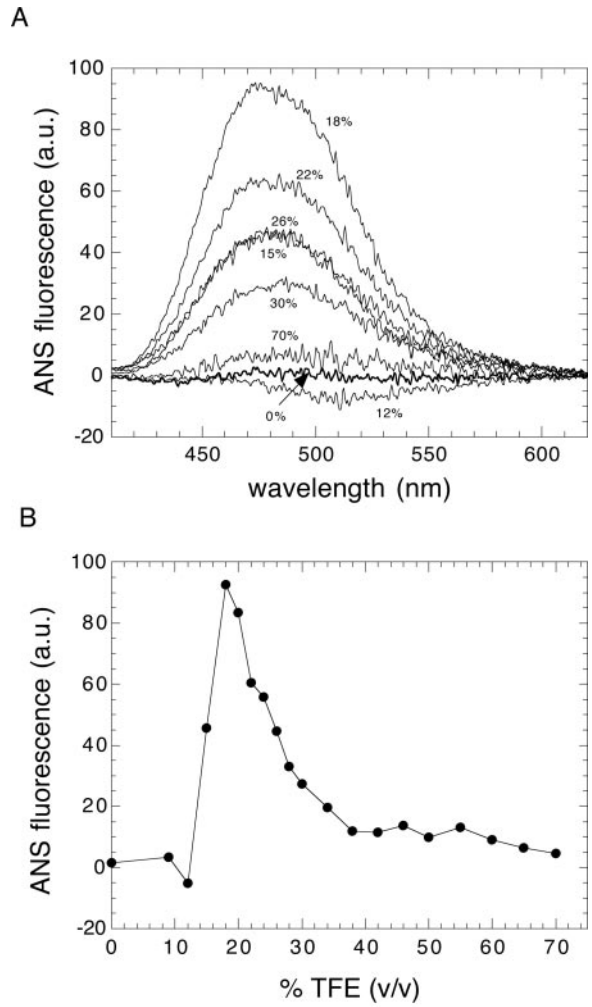

FIG. 2. **Fluorescence emission of ANS upon binding to Sso AcP pre-incubated in various TFE concentrations.** The protein samples were incubated for 30 min at 25 °C, pH 5.5, at the indicated TFE concentrations. *A* reports representative spectra of ANS obtained in the presence of Sso AcP pre-incubated at the indicated TFE concentrations. *B* reports the fluorescence emission of ANS at the observed maximum intensity (480 nm) as a function of TFE concentration. The spectra and values reported in the two panels were obtained by subtracting the spectra or values of ANS measured in the absence of protein at the corresponding TFE concentrations. *a.u.,* arbitrary units.

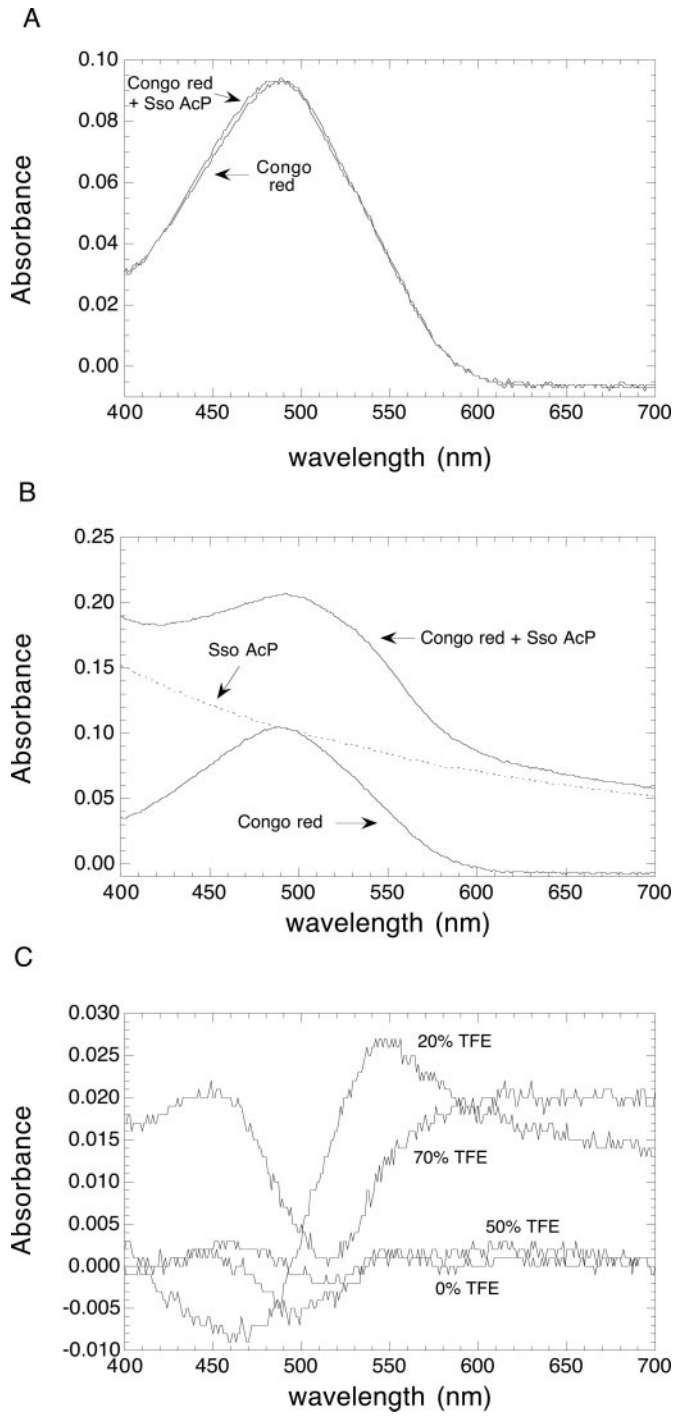

FIG. 3. **Congo red spectra in the presence and absence of protein pre-incubated in 0 (*A*) and 20% (*B*) TFE.** The spectrum obtained using Sso AcP alone pre-incubated in 20% (v/v) TFE is also displayed in *B* (*dotted line*). The spectrum of the 5 mM phosphate buffer, 150 mM NaCl, pH 7.4, was subtracted from all the other monitored spectra. *C* shows the difference spectra in various TFE concentrations, obtained by subtracting the spectra of the protein alone and of Congo red alone from the spectra of the protein in the presence of Congo red. The peak around 540 nm suggests ordered aggregates. The difference spectra represent the spectra of aggregate-bound Congo red. All protein samples were incubated for 30 min at 25 °C, pH 5.5, before the analysis.

(v/v) for 30 min at 25 °C, pH 5.5. Fig. 4 shows the size distribution by intensity recorded for two representative samples pre-incubated in 0 and 20% (v/v) TFE. Aggregates with an apparent diameter of ~200 nm were present in 20% TFE (Fig. 4, *dotted line*). On the contrary, a peak at ~3.4 nm was present in the protein samples in 0% TFE along with other larger particles (Fig. 4, *solid line*). The 3.4 nm diameter is highly consistent with that determined for proteins of the acylphosphatase superfamily using NMR or x-ray crystallography (22, 23, 24), suggesting that this peak arises from the native monomer.

Since the intensity of the scattered light is proportional to the sixth power of the size of the light-scattering particle, the size distribution by intensity is not indicative of the relative quantities of the detected species (39). When large particles are present in solution, peaks are detected from these particles even though they are of a negligible quantity. Therefore an additional mathematical analysis using Mie's theory was applied to yield the size distribution by volume (39) (Fig. 4, *inset*). This analysis, which conveys a more realistic description of the relative quantities of the various molecules present in solution, clearly showed that the native protein was by far the most represented species in 0% TFE. However, the presence of small amounts of aggregates in a sample with no TFE, analyzed just after centrifugation, indicated an intrinsic tendency of this protein to aggregate even in the absence of TFE. Size distributions by intensity and volume recorded in 10% (v/v) TFE were

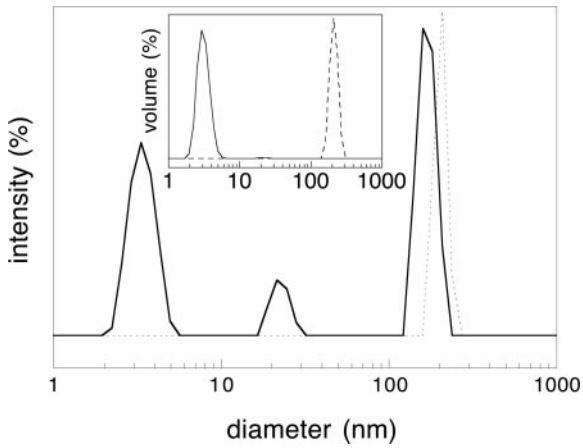

FIG. 4. **Size distribution by intensity of Sso AcP in 0 and 20% (v/v) TFE.** Sso AcP was incubated for 30 min in 0 or 20% (v/v) TFE at 25 °C, pH 5.5. The *continuous* and *dotted lines* refer to 0 and 20% TFE, respectively. The *inset* illustrates the size distribution by volume, which is a mathematical analysis obtained from the distribution by intensity. This represents more realistically the relative quantities of the molecules in a solution. The size distribution of Sso AcP in 0% TFE was obtained after centrifugation to remove very small amounts of large particles that masked the presence of the others.

similar to those obtained in 0% TFE (data not shown). At concentrations of TFE of 15% (v/v) or higher, only aggregated species were detected, even after centrifugation of the samples (data not shown).

Aggregate Formation Monitored by Electron Microscopy—The aggregates formed after 1 h at 25 °C in the presence of 20% (v/v) TFE were observed under transmission electron microscopy. The specimen revealed the presence of large amounts of small aggregates that filled up the background of the Formvar and carbon-coated grid (Fig. 5*A*). The smallest aggregates that we could identify had the appearance of spheres or short and thin fibrils with diameters of 3–5 nm (Fig. 5*A*, *inset*). These species appeared to be largely represented. The *arrows* in the *inset* of Fig. 5*A* indicate some of the thin fibrils. The morphology and the size of these structures are reminiscent of the cytotoxic precursor aggregates that precede formation of amyloid fibrils and that are often referred to as protofibrils (40, 41). Other aggregates were larger (diameter of up to 13 nm). One possibility is that they were assemblies of the smaller species. The specimen also revealed the presence of amorphous and very big clusters of aggregates (Fig. 5*A*). These are likely to be the aggregates with a size of ~200 nm that were detectable by DLS. As mentioned above, the intensity of the light scattered by a particle in solution is proportional to the sixth power of its size. Such big aggregates could therefore mask, in the DLS analysis, the small protofibrils that were present in solution.

Aggregates with a morphology similar to those obtained in 20% TFE after 1 h were also formed in the absence of TFE after several days (Fig. 5*B*). This demonstrates that Sso AcP may also form aggregates in the absence of TFE when the native state displays maximum stability. The observation that moderate concentrations of TFE are able to induce aggregation more rapidly is largely attributable to the ability of this fluoroalcohol to accelerate the aggregation process intrinsically, as indicated by studies carried out on unstructured or natively unfolded proteins (30, 42).

Aggregate Formation Monitored by Far-UV CD—Far-UV CD spectra of Sso AcP were acquired after incubation of the protein under different concentrations of TFE at pH 5.5, 25 °C (Fig. 6). In 0 and 10% (v/v) TFE, Sso AcP displayed similar spectra. These were typical of an α/β-structure and similar to that of other acylphosphatases previously characterized in their native state (43). In 20 and 25% (v/v) TFE, no CD signal was attained, probably due to the considerable scatter of the light at these wavelengths. In 50 and 70% (v/v) TFE, the two negative ellipticity bands at 208 and 222 nm indicated an α-helical structure. This was probably due either to oligomeric species that may potentially have had a substantial content of α-helical structure or to non-oligomeric conformations in equilibrium with the aggregated structures.

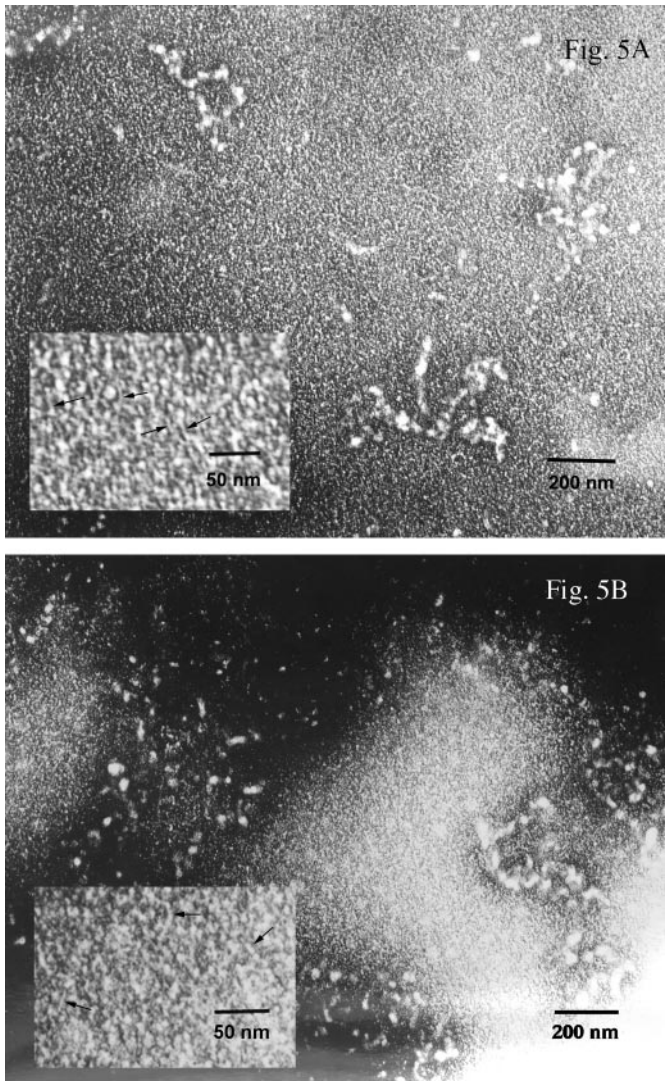

FIG. 5. **Electron micrographs of negatively stained Sso AcP aggregates formed in 20% (v/v) TFE after 1 h (*A*) and in the absence of TFE after 3 weeks (*B*) at 25 °C.** Small aggregates consisting of globules and short and thin fibrils are visible throughout the samples and form the background of the grids. These are often referred to as protofibrils and are thought to be the cytotoxic species in neurodegenerative pathologies. The presence of large aggregates is evident as well. The magnification was ×30,000. The *insets* illustrate more clearly the morphology of the protofibrillar structures. *Arrows* indicate elongated protofibrils with an approximate diameter of 3–5 nm.

Determination of the Rate of Aggregation—The rate of aggregation of Sso AcP was evaluated in various TFE concentrations. Aggregation was followed in the presence of 20% (v/v) TFE using ThT fluorescence at 485 nm, ANS fluorescence at 480 nm, and far-UV CD at 222 nm (Fig. 7). Whereas ThT and ANS fluorescence increased as the aggregates formed, the far-UV CD signal decreased as the protein converted from a soluble form with a CD signal to an aggregated form with no signal (Fig. 7). From all techniques, the process of aggregation seemed to follow single exponential kinetics with rate constants that

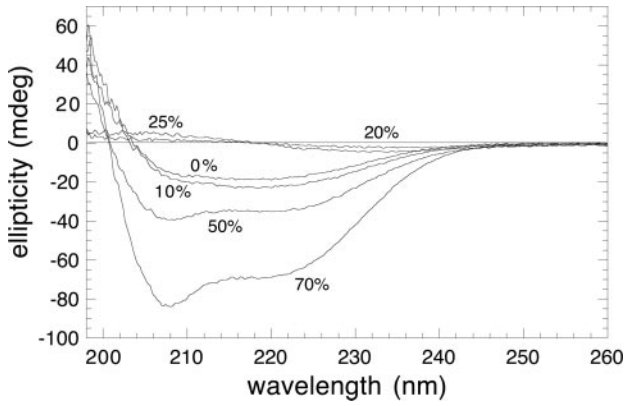

FIG. 6. **Far-UV CD spectra of Sso AcP pre-incubated under different TFE concentrations.** Spectra were recorded after pre-incubation of Sso AcP for 30 min at pH 5.5, 25 °C, at the indicated concentrations of TFE. All spectra shown in the figure were obtained after subtraction of the spectrum recorded with buffer from all the acquired spectra. Due to significant light scattering originating from the aggregates, the spectra were not converted to mean residue ellipticity units.

were, within experimental error, similar to each other (0.0045 ± 0.0002, 0.0058 ± 0.0007, and 0.0037 ± 0.0005 s^{-1}, respectively). The rate of aggregation increased with increasing amounts of TFE. From the analysis performed with ThT, the observed rate constants were 0.0010 ± 0.0002 s^{-1} in 15%, 0.0045 ± 0.0007 s^{-1} in 20%, and 0.011 ± 0.002 s^{-1} in 25% (v/v) TFE. In the presence of 50 and 70% (v/v) TFE, aggregation was too rapid to be measured accurately, with the ThT fluorescence reaching the plateau before the first measurement.

Determination of the Conformational State of Sso AcP Under Conditions Favoring Aggregation—One important issue to address was the conformational state adopted by soluble Sso AcP before aggregation occurs. This was done by evaluating the enzymatic activity of Sso AcP in various concentrations of TFE (Fig. 8). In a first set of experiments, Sso AcP was incubated for 30 min in different TFE concentrations before the measurement of the resulting enzymatic activity, which was estimated in each case under the same pre-incubation conditions. The decrease of the enzymatic activity was minimal from 0 to 12% (v/v) TFE (Fig. 8, *filled circles*). At TFE concentrations higher than 12% (v/v), the activity diminished abruptly reaching a value close to zero beyond 18% (v/v) TFE. On the contrary, when activity was measured without previous incubation in TFE, substantial activity was observed until 26% (v/v) TFE (Fig. 8, ×). The detection of enzymatic activity was indicative of the presence of native-like Sso AcP under these conditions when the aggregation process is far from completion. The activity of the samples without previous pre-incubation was found to be 50–60% that measured in the absence of TFE. This may lead to the possibilities that the aggregation process had partially started when activity was measured in the presence of TFE, that TFE lowered the catalytic efficiency of the protein intrinsically, or that the protein went through slight structural modifications under these solvent conditions. An enzymatic activity reduced to a value of 50–60% may also be due, in principle, to an equilibrium between the native and the denatured states, with only half of the protein adopting a native conformation. However, folding and unfolding rate measurements allowed this possibility to be discarded (see below).

To rule out the possibility that the residual activity in the experiments described above was observed due to lack of time for the protein to denature, Sso AcP was incubated in 6 M GdnHCl for 30 min before the activity measurement. Preliminary results have shown that incubation of Sso AcP in 6 M GdnHCl for this length of time is sufficient to allow full denaturation and activity suppression of the protein (data not shown). Upon removal of GdnHCl, enzymatic activity was recovered in the presence of TFE concentrations up to 26% (v/v) TFE, reaching levels similar to those observed without previous denaturation of the protein in GdnHCl (Fig. 8, *open circles*). This indicated that under these concentrations of TFE, the protein existed in an enzymatically active conformation before aggregation occurred.

To investigate further the conformational state of Sso AcP

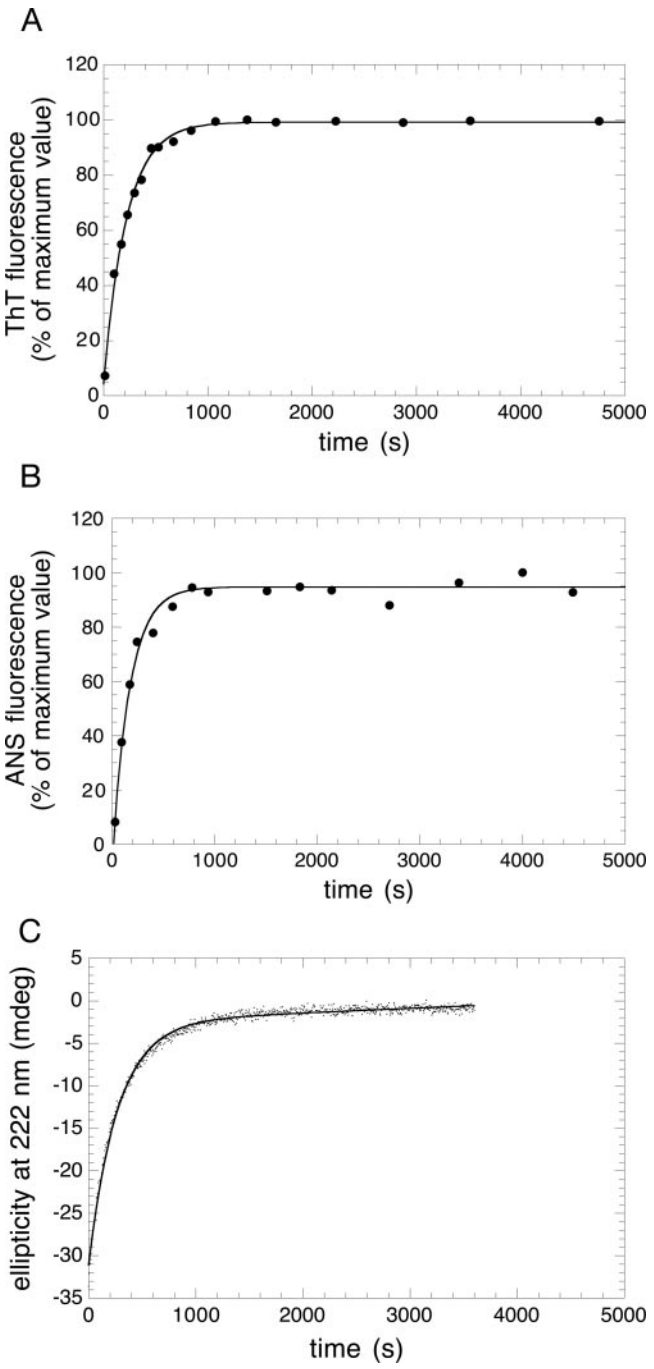

FIG. 7. **Spectroscopic changes during aggregation of Sso AcP.** Aggregation was monitored at a protein concentration of 0.4 mg/ml, 20% (v/v) TFE, 50 mM acetate buffer, pH 5.5, 25 °C. *A*, increase of ThT fluorescence at 485 nm. *B*, increase of ANS fluorescence at 480 nm. *C*, decrease of ellipticity at 222 nm. The values reported in the figure were obtained by subtracting, from the observed values, the corresponding values of ThT fluorescence, ANS fluorescence, and ellipticity recorded in the absence of protein.

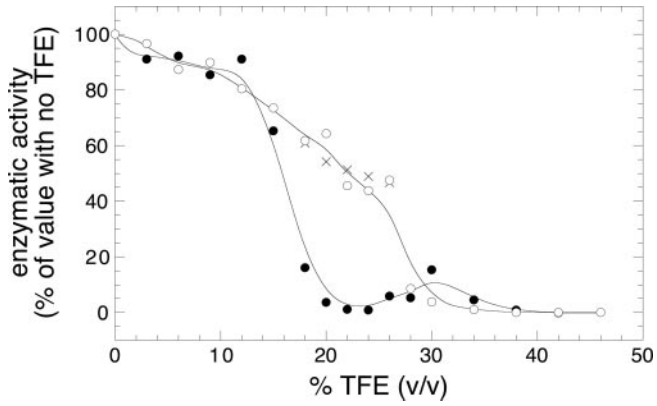

FIG. 8. **Enzymatic activity of Sso AcP under different concentrations of TFE.** The protein was pre-incubated for 30 min in 50 mM acetate buffer, pH 5.5, 25 °C, in the absence of TFE (×), in the presence of different concentrations of TFE (*filled circles*), and in the presence of 6 M GdnHCl (*empty circles*). After pre-incubation, acylphosphatase activity was measured at the concentrations of TFE indicated in the figure. In the set of experiments with pre-incubation in TFE, the same concentrations of fluoroalcohol were maintained in the pre-incubation samples and during activity measurements. All activity values reported in the figure were obtained after subtracting the spontaneous hydrolysis of substrate determined in the absence of protein under the corresponding TFE concentrations. *Solid lines* simply represent trend lines.

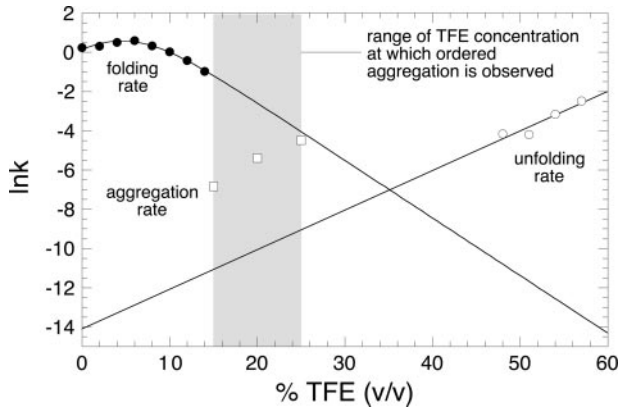

FIG. 9. **Natural logarithm of folding and unfolding rate of Sso AcP as a function of TFE concentration.** Measurements were performed at pH 5.5, 25 °C. Folding rate (*filled circles*) and unfolding rate (*open circles*) data points were fitted to the equation previously described (43) and to a linear equation, respectively. Aggregation rate values in logarithmic form obtained in 15, 20, and 25% (v/v) TFE are also reported (*open squares*). The *gray area* represents the range of TFE concentration in which ordered aggregates able to bind ThT, ANS, and Congo red are formed.

before aggregation, the folding and unfolding rates of Sso AcP were measured under different concentrations of TFE (Fig. 9). Similarly to other single-domain proteins, unfolding of Sso AcP is a monophasic process with a single major energy barrier.[2] The unfolding rate was measured at concentrations of TFE higher than 45% (v/v) as protein aggregation obscured spectroscopically the unfolding process at lower TFE concentrations (Fig. 9). Folding of Sso AcP is a multiphasic process in which the unfolded state first collapses very rapidly into a partially folded state before folding to the native state with the same energy barrier as that observed for unfolding.[2] The rate of conversion of the partially folded state into the native state was determined at concentrations of TFE lower than 15% (Fig. 9). Due to the same technical difficulties encountered for unfolding, kinetic profiles were not interpretable at higher TFE concentrations. The rate of Sso AcP folding has the characteristic bell-shaped dependence on TFE concentration that was described for several other proteins (44).

Although the folding and unfolding rates could not be determined directly under the conditions in which ordered aggregation was observed to occur rapidly (15–25% (v/v) TFE), the rate values under these conditions were obtained by extrapolating the values obtained in ranges of TFE concentrations of 0–15 and 45–60% (v/v), respectively (Fig. 9). Most interesting, the unfolding rate extrapolated to zero TFE concentration was in close agreement with that obtained from the Chevron plot obtained using GdnHCl as a denaturant,[2] indicating the correctness of the linear extrapolation used here. The analysis showed that folding was faster than unfolding throughout the TFE concentration range of 15–25% (v/v) (Fig. 9). This implies that the native state was thermodynamically more stable than the partially folded state under these conditions, therefore representing the majority of the Sso AcP molecules before aggregate formation. Perhaps the most important observation to emphasize here is that aggregation was also faster than unfolding under these conditions (*cf. open squares* with extrapolation line for unfolding in Fig. 9).

[2] F. Bemporad, C. Capanni, M. Calamai, M. L. Tutino, M. Stefani, and F. Chiti, unpublished results.

DISCUSSION

Aggregation of Sso AcP May Occur from a Folded Conformation—The results presented in this paper reveal that in the presence of 15–25% TFE Sso AcP converts rapidly into protofibrillar aggregates that have the ability to bind dyes such as Congo red, ThT, and ANS (Figs. 1–5). These protofibrillar aggregates appear to be sticky and to assemble further to generate large clusters with an apparent hydrodynamic diameter of up to 200 nm, as revealed by DLS (Fig. 4). Given their tendency to assemble, these aggregates are not detectable with far-UV CD as a consequence of the substantial scattering of the light at these wavelength values (Fig. 6).

Prior to aggregation Sso AcP adopts a conformational state, under these conditions, that retains a considerable acylphosphatase activity (Fig. 8). The acylphosphatase activity of human muscle acylphosphatase, a protein belonging to the same structural superfamily as Sso AcP, is ensured by a precise three-dimensional positioning of residues such as the 15–21 catalytic loop, the arginine at position 23, and the asparagine at position 41 (45). Mutations that are distant from the active site can reduce the enzymatic activity substantially with no apparent change of the native structure as detected with one-dimension NMR (46). The ability of Sso AcP to function as an active enzyme in 15–25% TFE is therefore suggestive of a folded conformation with possibly only minor structural modifications relative to the native state. Within this range of TFE concentrations, unfolding of Sso AcP appears to be slower than the conversion of the partially folded state into the native state (Fig. 9). This indicates that, under these conditions, the native state is thermodynamically favored over the unfolded or partially unfolded states, as can be expected from a hyperthermophilic protein. Moreover, Sso AcP unfolding is very slow under these conditions, denoting that it adopts a structure that retains a close packing of residues and lies on the "folded side" of the major free energy barrier for (un)folding. Although we cannot rule out that the conformation adopted by Sso AcP under these conditions is a slightly distorted form of the fully native state, the data show that such structural modifications are only minor.

The finding that aggregation is nearly 100 times faster than unfolding within this range of TFE concentrations (Fig. 9) indicates that self-assembly of Sso AcP does not require a transition of the protein molecules into a partially unfolded

state. Aggregation occurs from protein molecules that adopt a native-like topology. Since we have not yet carried out a structural investigation of the aggregates formed under these conditions, we cannot establish whether the individual protein molecules adopt a native-like topology or a substantially different structure in the resulting aggregates. Indeed, the results shown here only report evidence that aggregation may involve a mechanistic assembly of molecules in their native topology; substantial structural reorganization may occur as a consequence of the formation of the first intermolecular interactions. The ability of these aggregates to bind and increase the fluorescence of ANS, in contrast to the non-aggregated state under these conditions, suggests that this is the case.

Aggregation is also observed in the absence of TFE (Fig. 5*B*). The intrinsic ability of TFE to accelerate aggregation of polypeptide chains (30, 42) explains why this fluoroalcohol is needed to induce rapid aggregation of Sso AcP. Indeed, studies carried out using the natively unfolded proteins Aβ and α-synuclein have shown that in the presence of moderate concentrations of TFE, aggregation is substantially faster than in their absence (30, 42). In addition, structural distortions that may occur locally in the native Sso AcP in the presence of TFE concentrations as high as 15–25% (v/v) may contribute to facilitate aggregation.

Aggregation from Folded States Versus Aggregation from Partially Unfolded States, a Unifying Picture—These results do not contradict the view that partial unfolding favors and is generally required for aggregation. Indeed, in the presence of 50 and 70% (v/v) TFE, aggregation of Sso AcP is much faster than in 15–25% (v/v) TFE. In 50–70% TFE, the denatured state of Sso AcP is thermodynamically favored over the native state (Fig. 9), and enzymatic activity is absent at TFE concentrations higher than 40% (Fig. 8). Aggregation occurs also under these conditions, as revealed by DLS and a significant ThT binding (Figs. 1 and 4). The process appears, however, to be very fast. The relatively weak ThT binding and the absence of Congo red and ANS binding probably result from the rapidity of the aggregation process under these conditions, which leads to the formation of relatively disordered aggregates (Figs. 1–3).

The rapidity of the aggregation process of Sso AcP at high, relative to moderate, TFE concentrations does not result from the ability of TFE to accelerate aggregation intrinsically. In fact, from studies carried out using the natively unfolded proteins Aβ and α-synuclein, it is clear that in 50–70% TFE, aggregation is slower than in the presence of 15–25% (30, 42). The faster aggregation of Sso AcP at high TFE concentrations is thus attributable to the fact that the protein no longer maintains a folded structure. Aggregation of Sso AcP may therefore possibly start from both a folded conformation and a denatured state but with different rates (Fig. 10). Although aggregation may still occur from a folded state, self-assembly is kinetically favored under conditions in which partially unfolded states are populated (Fig. 10). This is in agreement with a large body of data showing that mutations able to destabilize the native state of a globular protein facilitate aggregation (20, 21, 47–54). It is also in agreement with several observations that partially denaturing conditions are required to start aggregation for proteins that normally adopt a folded structure (1, 5, 6, 19).

Conclusions—The utilization of a stable protein from a hyperthermophilic Archaea has allowed aggregation to be studied under destabilizing conditions that are known to favor this process while maintaining, or altering only slightly, the native structure of the protein due to its high conformational stability. The data indicate that aggregation may occur from either a folded structure or a denatured state, depending on conditions.

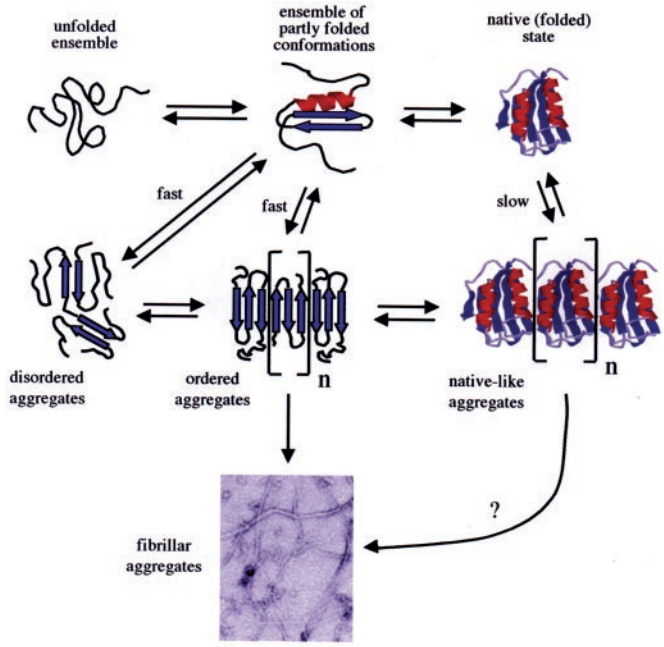

FIG. 10. **Possible pathways to aggregation.** A globular protein adopting a folded structure can give rise to protein aggregates by partially unfolding before assembly or directly from the native state. Aggregation from an ensemble of partially folded conformations is faster than from the folded state. However, the latter process may be significant as a globular protein spends most if its lifetime in a folded conformation.

Although the latter process is kinetically favored *per se*, the slower aggregation process that is due to conformations close to the native state may have a higher physiological relevance. In fact, proteins normally live under non-denaturing environments in which such states are by far more populated than others. Aggregation is protein concentration-dependent, and the apparently slower aggregation process from the folded conformations may become kinetically favored if one considers that such species are far more represented than partially unfolded ones.

These results are in agreement with findings that proteins such as the yeast prion Ure2p and human lithostatin may form fibrillar aggregates without an extensive cross-β structure and with a native-like content of secondary structure (13, 14). They also fit with indications that natural β-sheet proteins have evolved with structural adaptations that impede assembly of protein molecules in their native conformations via edge to edge interaction of β-sheets (55). Indeed, such adaptations are reminiscent of the potential of proteins to aggregate from their folded states. Finally, common structural features inherent to the native structure have been identified for globular proteins that form amyloid fibrils naturally in pathological conditions (56). All these findings will contribute to shift the focus of our attention from partially unfolded or misfolded conformations to the native state for an understanding of aggregation processes that are physiologically relevant and occur naturally in living organisms.

Acknowledgments—We thank Luisa Tutino for providing the gene of Sso AcP. We also thank Patrizio Guasti and Maria Giuliana Vannucchi for their technical assistance with transmission electron microscopy.

REFERENCES

1. Stefani, M., and Dobson, C. M. (2003) *J. Mol. Med.* **81,** 678–699
2. Sunde, M., and Blake, C. (1997) *Adv. Protein Chem.* **50,** 123–159
3. Kelly, J. W. (1998) *Curr. Opin. Struct. Biol.* **8,** 101–106
4. Rochet, J. C., and Lansbury, P. T., Jr. (2000) *Curr. Opin. Struct. Biol.* **10,** 60–68
5. Lai, Z., Colon, W., and Kelly, J. W. (1996) *Biochemistry* **35,** 6470–6482

6. McParland, V. J., Kalverda, A. P., Homans, S. W., and Radford, S. E. (2002) *Nat. Struct. Biol.* **9,** 326–331
7. Hoshino, M., Katou, H., Hagihara, Y., Hasegawa, K., Naiki, H., and Goto, Y. (2002) *Nat. Struct. Biol.* **9,** 332–336
8. Rousseau, F., Schymkowitz, J. W., Wilkinson, H. R., and Itzhaki, L. S. (2001) *Proc. Natl. Acad. Sci. U. S. A.* **98,** 5596–5601
9. Staniforth, R. A., Giannini, S., Higgins, L. D., Conroy, M. J., Hounslow, A. M., Jerala, R., Craven, C. J., and Waltho, J. P. (2001) *EMBO J.* **20,** 4774–4781
10. Petkova, A. T., Ishii, Y., Balbach, J. J., Antzutkin, O. N., Leapman, R. D., Delaglio, F., and Tycko, R. (2002) *Proc. Natl. Acad. Sci. U. S. A.* **99,** 16742–16747
11. Torok, M., Milton, S., Kayed, R., Wu, P., McIntire, T., Glabe, C. G., and Langen, R. (2002) *J. Biol. Chem.* **277,** 40810–40815
12. Lopez de La Paz, M., Goldie, K., Zurdo, J., Lacroix, E., Dobson, C. M., Hoenger, A., and Serrano, L. (2002) *Proc. Natl. Acad. Sci. U. S. A.* **99,** 16052–16057
13. Bousset, L., Thomson, N. H., Radford, S. E., and Melki, R. (2002) *EMBO J.* **17,** 2903–2911
14. Laurine, E., Gregoire, C., Fandrich, M., Engemann, S., Marchal, S., Thion, L., Mohr, M., Monsarrat, B., Michel, B., Dobson, C. M., Wanker, E., Erard, M., and Verdier, J. M. (2003) *J. Biol. Chem.* **278,** 51770–51778
15. Taylor, K. L., Cheng, N., Williams, R. W., Steven, A. C., and Wickner, R. B. (1999) *Science* **283,** 1339–1343
16. Thual, C., Komar, A. A., Bousset, L., Fernandez-Bellot, E., Cullin, C., and Melki, R. (1999) *J. Biol. Chem.* **274,** 13666–13674
17. Thual, C., Bousset, L., Komar, A. A., Walter, S., Buchner, J., Cullin, C., and Melki, R. (2001) *Biochemistry* **40,** 1764–1773
18. Bousset, L., Briki, F., Doucet, J., and Melki, R. (2003) *J. Struct. Biol.* **141,** 132–142
19. Guijarro, J. I., Sunde, M., Jones, J. A., Campbell, I. D., and Dobson, C. M. (1998) *Proc. Natl. Acad. Sci. U. S. A.* **95,** 4224–4228
20. Chiti, F., Taddei, N., Bucciantini, M., White, P., Ramponi, G., and Dobson, C. M. (2000) *EMBO J.* **19,** 1441–1449
21. Ramirez-Alvarado, M., Merkel, J. S., and Regan, L. (2000) *Proc. Natl. Acad. Sci. U. S. A.* **97,** 8979–8984
22. Pastore, A., Saudek, V., Ramponi, G., and Williams, R. J. (1992) *J. Mol. Biol.* **224,** 427–440
23. Thunnissen, M. M., Taddei, N., Liguri, G., Ramponi, G., and Nordlund, P. (1997) *Structure* **5,** 69–79
24. Rosano, C., Zuccotti, S., Bucciantini, M., Stefani, M., Ramponi, G., and Bolognesi, M. (2002) *J. Mol. Biol.* **321,** 785–796
25. Camici, G., Manao, G., Cappugi, G., and Ramponi, G. (1976) *Experientia* (*Basel*) **32,** 535–536
26. Taddei, N., Stefani, M., Magherini, F., Chiti, F., Modesti, A., Raugei, G., and Ramponi, G. (1996) *Biochemistry* **35,** 7077–7083
27. Bucciantini, M., Giannoni, E., Chiti, F., Baroni, F., Formigli, L., Zurdo, J., Taddei, N., Ramponi, G., Dobson, C. M., and Massimo, S. (2002) *Nature* **416,** 507–511
28. Srisailam, S., Kumar, T. K., Rajalingam, D., Kathir, K. M., Sheu, H. S., Jan, F. J., Chao, P. C., and Yu, C. (2003) *J. Biol. Chem.* **278,** 17701–17709
29. Barrow, C. J., and Zagorski, M. G. (1991) *Science* **253,** 179–182
30. Fezoui, Y., and Teplow, D. B. (2002) *J. Biol. Chem.* **277,** 36948–36954
31. Chiti, F., Stefani, M., Taddei, N., Ramponi, G., and Dobson, C. M. (2003) *Nature* **424,** 805–808
32. Goldberg, M. S., and Lansbury, P. T (2000) *Nat. Cell Biol.* **2,** E115–E119
33. Sousa, M. M., Cardoso, I., Fernandes, R., Guimaraes, A., and Saraiva, M. J. (2001) *Am. J. Pathol.* **159,** 1993–2000
34. Walsh, D. M., Klyubin, I., Fadeeva, J. V., Cullen, W. K., Anwyl, R., Wolfe, M. S., Rowan, M. J., and Selkoe, D. J. (2002) *Nature* **416,** 535–539
35. LeVine, H., III (1999) *Methods Enzymol.* **309,** 274–284
36. Semisotnov, G. V., Rodionova, N. A., Razgulyaev, O. I., Uversky, V. N., Gripacæ, A. F., and Gilmanshin, R. I. (1991) *Biopolymers* **31,** 119–128
37. Kremer, J. J., Pallitto, M. M., Sklansky, D. J., and Murphy, R. M. (2000) *Biochemistry* **39,** 10309–10318
38. Klunk, W. E., Pettegrew, J. W., and Abraham, D. J. (1989) *J. Histochem. Cytochem.* **37,** 1273–1281
39. van de Hulst, H. C. (1957) *Light Scattering by Small Particles*, pp. 1–80, John Wiley & Sons, Inc., New York
40. Harper, J. D., Wong, S. S., Lieber, C. M., and Lansbury, P. T. (1997) *Chem. Biol.* **4,** 119–125
41. Conway, K. A., Lee, S. J., Rochet, J. C., Ding, T. T., Williamson, R. E., and Lansbury, P. T., Jr. (2000) *Proc. Natl. Acad. Sci. U. S. A.* **97,** 571–576
42. Munishkina, L. A., Phelan, C., Uversky, V. N., and Fink, A. L. (2003) *Biochemistry* **42,** 2720–2730
43. Chiti, F., Taddei, N., Webster, P., Hamada, D., Fiaschi, T., Ramponi, G., and Dobson, C. M. (1999) *Nat. Struct. Biol.* **6,** 380–387
44. Hamada, D., Chiti, F., Guijarro, J. I., Kataoka, M., Taddei, N., and Dobson, C. M. (2000) *Nat. Struct. Biol.* **7,** 58–61
45. Stefani, M., Taddei, N., and Ramponi, G. (1997) *Cell. Mol. Life Sci.* **53,** 141–151
46. Taddei, N., Magherini, F., Chiti, F., Bucciantini, M., Raugei, G., Stefani, M., and Ramponi, G. (1996) *FEBS Lett.* **384,** 172–176
47. Hurle, M. R., Helms, L. R., Li, L., Chan, W., and Wetzel, R. (1994) *Proc. Natl. Acad. Sci. U. S. A.* **91,** 5446–5450
48. Funahashi, J., Takano, K., Ogasahara, K., Yamagata, Y., and Yutani, K. (1996) *J. Biochem.* (*Tokyo*) **120,** 1216–1223
49. Booth, D. R., Sunde, M., Bellotti, V., Robinson, C. V., Hutchinson, W. L., Fraser, P. E., Hawkins, P. N., Dobson, C. M., Radford, S. E., Blake, C. C. F., and Pepys, M. B. (1997) *Nature* **385,** 787–793
50. Raffen, R., Dieckman, L. J., Szpunar, M., Wunschl, C., Pokkuluri, P. R., Dave, P., Wilkins Stevens, P., Cai, X., Schiffer, M., and Stevens, F. J. (1999) *Protein Sci.* **8,** 509–517
51. Quintas, A., Vaz, D. C., Cardoso, I., Saraiva, M. J., and Brito, R. M. (2001) *J. Biol. Chem.* **276,** 27207–27213
52. Canet, D., Last, A. M., Tito, P., Sunde, M., Spencer, A., Archer, D. B., Redfield, C., Robinson, C. V., and Dobson, C. M. (2002) *Nat. Struct. Biol.* **9,** 308–315
53. Hammarstrom, P., Jiang, X., Hurshman, A. R., Powers, E. T., and Kelly, J. W. (2002) *Proc. Natl. Acad. Sci. U. S. A.* **99,** 16427–16432
54. Smith, D. P., Jones, S., Serpell, L. C., Sunde, M., and Radford, S. E. (2003) *J. Mol. Biol.* **330,** 943–954
55. Richardson, J. S., and Richardson, D. C. (2002) *Proc. Natl. Acad. Sci. U. S. A.* **99,** 2754–2759
56. Fernandez, A., Kardos, J., Scott, L. R., Goto, Y., and Berry, R. S. (2003) *Proc. Natl. Acad. Sci. U. S. A.* **100,** 6446–6451

Aggregation of the Acylphosphatase from *Sulfolobus solfataricus*: THE FOLDED AND PARTIALLY UNFOLDED STATES CAN BOTH BE PRECURSORS FOR AMYLOID FORMATION

Georgia Plakoutsi, Niccolò Taddei, Massimo Stefani and Fabrizio Chiti

J. Biol. Chem. 2004, 279:14111-14119.
doi: 10.1074/jbc.M312961200 originally published online January 14, 2004
